Chapter 2

The effects of Faraday rotation on polarization in electron-scattering atmospheres

2.1 Introduction

Discussions of polarization as it relates to accretion disks in AGN are problematic when one considers the possibility that the disks have magnetic fields which are in equipartition with the thermal energy of the disk interior. As suggested by a number of authors (Gnedin and Silant'ev 1978; Blandford 1990; Matt, Fabian, and Ross 1993; Begelman 1994; Blandford and Lee 1997), Faraday rotation might then dramatically alter the optical/UV polarization. Indeed, the equipartition magnetic field in the inner regions of a disk around a Schwarzschild hole in the standard Novikov and Thorne (1973) model is

$$B \simeq 1 \times 10^5 \text{Gauss}\ \alpha^{-1/2} \left(\frac{M}{10^8\ \mathrm{M}_\odot}\right)^{-1/2} \left(\frac{r}{r_\mathrm{g}}\right)^{-3/4}, \tag{2.1}$$

where r is the Schwarzschild radial coordinate, $r_\mathrm{g} \equiv GM/c^2$ is the gravitational radius, M is the mass of the hole, and α is the viscosity parameter.[1] This

[1]Novikov and Thorne (1973) assume that the magnetic energy density can be at most the viscous stress in their estimates of the field strength (due to shearing of the field), resulting in a maximum field strength which is a factor $(3/\alpha)^{1/2}$ times smaller than our equation (2.1).

formula assumes that the fields can be in equipartition with the total (i.e. radiation) thermal energy density, which is appropriate if the photon mean free paths are short compared to the disk scale height so that the radiation and plasma truly behave as a single fluid. Magnetic fields can in principle produce severe Faraday rotation at optical and UV wavelengths λ. The expected Faraday rotation angle would be $\simeq 0.1\tau_{\rm T}B_{\parallel}(\lambda/5000\text{Å})^2$ radians, where $\tau_{\rm T} \sim 1$ is the Thomson depth along the line of sight near the scattering photosphere, and $B_{\parallel}$ is the magnetic field component (in G), also along the line of sight. Clearly if the field at the photosphere is anywhere near the strength given by equation (2.1), the Faraday rotation is severe and would completely depolarize the radiation field.

There are compelling theoretical arguments that accretion disks in AGN are strongly magnetized. The turbulence required to transport angular momentum outward combined with the strong differential rotation is a natural site for a dynamo (e.g. Pudritz 1981). Even if the flow were laminar, a weak field would catalyze angular momentum transport and produce an instability whereby it would grow in strength at the expense of the free energy stored in differential rotation (Balbus and Hawley 1991). In the case of AGN, accreting material can advect poloidal field inwards from the interstellar medium. This field could then simply be stretched and amplified into toroidal field, again by the differential rotation (e.g. Field and Rogers 1994). Each of these scenarios would lead to a strong field. Dynamos would be expected to build up field to be in equipartition with the turbulent velocity field. Recent simulations of the Balbus-Hawley instability by Stone et al. (1996) produce a magnetic energy density which is several percent of the thermal energy density at the disk midplane, but then the magnetic energy density increases with height to locally superequipartition values. Further simulations which include a better treatment of heating and cooling are still necessary to understand the distribution and strength of the field. In AGN, the field advected in from the interstellar medium could be suprathermal in strength (Field and Rogers 1994). Magnetic fields could be directly responsible for providing the required angular momentum transport in the disk, through both internal and/or external torques (e.g. Blandford 1990). They may provide the acceleration and collimation mechanism for jets (e.g. Blandford and Payne 1982; Chiueh, Li, and Begelman 1991), and may even

Note that the numerical coefficient of 7×10^7 G in their equation (5.9.10) is incorrect. It should be 4×10^8 G. These differences are all of course well within the theoretical uncertainties!

release the reducible mass-energy of the spinning black hole itself (Blandford and Znajek 1977). Magnetized coronae in two-phase accretion disk models are becoming increasingly popular for explaining the X-ray properties of AGN (e.g. Haardt and Maraschi 1993; Svensson and Zdziarski 1994). Given these arguments for the presence of a magnetic field, the role of Faraday rotation on the polarization of accretion disk radiation needs to be considered.

Detailed calculations of the effects of Faraday rotation on the polarization of radiation emerging from a plane-parallel, scattering atmosphere have been published by Silant'ev (1979) in the limit that the Faraday rotation for unit Thomson depth is large. These results were used to estimate the effect of Faraday rotation in homogeneous disks with constant magnetic field strength in X-ray binaries by Gnedin and Silant'ev (1977; 1978). They found that depolarization could be severe for large field strengths, with the degree of polarization $P \propto \lambda^{-2}$ at large wavelengths.

The aim of this chapter is to improve upon and generalize the basic results of Silant'ev (1979), and to apply them to simple AGN disk models. We compute the radiative transfer with Monte Carlo simulations and finite difference calculations. Our results cover the full range of magnetic effects, and bridge the results of Silant'ev (1979) with the nonmagnetic case of Chandrasekhar (1960). In section 2.2 we outline our basic assumptions and equations. We present our results for polarization of radiation emerging from plane-parallel, optically thick scattering slabs with both uniform and random magnetic fields in section 2.3. In section 2.4 we apply these results to various accretion disk models, and finally summarize our conclusions in section 2.5. In an appendix to this chapter, we rederive Silant'ev's results for strong Faraday depolarization using our notation.

2.2 Equations

2.2.1 Monte Carlo calculations

Our Monte Carlo code calculates the polarized radiation field emerging from a plane-parallel, magnetized atmosphere with pure electron scattering opacity. The code is based on the prescriptions for an unmagnetized atmosphere described by Angel (1969). Photons are injected isotropically into the bottom layer of a slab of large finite optical depth, and then tracked until they either emerge from the top or penetrate the bottom surface, in which case we simply

reflect them. (We also ran cases with a perfectly absorbing lower boundary condition, but as expected there is little difference in the results for large optical depths.) We have tested the code in the limit of zero magnetic field, and have successfully reproduced the optically thick analytic results of Chandrasekhar (1960) as well as the optically thin numerical results of Phillips and Mészáros (1986).

Transfer of polarized radiation through a magnetized plasma can be treated in nearly the same way as the nonmagnetized case for the regime in which we are interested. Consider the wave propagation modes through a cold plasma in a uniform magnetic field. We are interested in wave angular frequencies ω which are typically $\sim 3.8 \times 10^{15} (\lambda/5000\mathring{A})^{-1}$ rad s^{-1}. These are much higher than the characteristic frequencies of the plasma, in particular the electron cyclotron frequency $\omega_B = 1.8 \times 10^{11} (B/10^4 \mathrm{G})$ rad s^{-1} and the electron plasma frequency $\omega_\mathrm{p} = 1.8 \times 10^9 (n_\mathrm{e}/10^9 \mathrm{cm}^{-3})^{1/2}$ rad s^{-1}, where n_e is the electron number density. (Unless the "ions" are primarily positrons, the ion cyclotron and plasma frequencies are even lower.) It is well-known that in this high frequency limit, the modes may be approximated as circularly polarized vacuum electromagnetic waves. The electric field vectors are nearly transverse to the wave vector $\mathbf{k} = k\mathbf{n}$, with the ratio of parallel to perpendicular components being given by

$$\left| \frac{E_\parallel}{E_\perp} \right| \simeq \frac{\omega_\mathrm{p}^2 \omega_B}{\omega^3} |\sin\xi| \ll 1, \tag{2.2}$$

where ξ is the angle between the wave vector and the magnetic field. The dispersion relation for the right (R) and left (L) circularly polarized modes is

$$k_\mathrm{R,L} \simeq \frac{\omega}{c} \left(1 - \frac{\omega_\mathrm{p}^2}{2\omega^2} \pm \frac{\omega_\mathrm{p}^2 \omega_B}{2\omega^3} \cos\xi \right). \tag{2.3}$$

The third term of this dispersion relation represents the effects of Faraday rotation, and is the only plasma effect on the radiative transfer that is important to incorporate into the calculation. Hence in the Monte Carlo simulation we treat photons as transverse, linearly polarized waves which propagate at the speed of light between absorption and scattering, but whose plane of polarization undergoes Faraday rotation according to the local magnetic field along the propagation trajectory.

In the same high frequency limit, the differential Thomson cross section for

linearly polarized radiation is

$$\frac{d\sigma}{d\Omega} = r_0^2 \left[(\mathbf{p}' \cdot \mathbf{p})^2 + O\left(\frac{\omega_B^2}{\omega^2}\right) \right], \tag{2.4}$$

where r_0 is the classical electron radius and $\mathbf{p}$ and $\mathbf{p}'$ are the incident and scattered polarization vectors (normalized to unit magnitude). Since $\omega_B/\omega < 10^{-4}$ in our models, the effect of the magnetic field on the Thomson cross section is negligible.[2] The normalized angular distribution of scattered polarized light is then given by

$$f(\Omega) = \frac{3}{8\pi}(1 - \cos^2\theta), \tag{2.5}$$

where θ is the angle between the incident photon polarization $\mathbf{p}$ and the outgoing photon direction unit vector $\mathbf{n}'$. The distribution around $\mathbf{p}$ is axisymmetric, corresponding to a uniform distribution in azimuthal angle ϕ.

In terms of these scattering angles, the outgoing photon direction is given by

$$n_x' = \frac{p_y}{p_{xy}} \sin\theta\cos\phi + \frac{p_x p_z}{p_{xy}} \sin\theta\sin\phi + p_x\cos\theta \tag{2.6}$$

$$n_y' = -\frac{p_x}{p_{xy}} \sin\theta\cos\phi + \frac{p_y p_z}{p_{xy}} \sin\theta\sin\phi + p_y\cos\theta \tag{2.7}$$

and

$$n_z' = p_{xy}\sin\theta\sin\phi + p_z\cos\theta, \tag{2.8}$$

where $p_{xy} = \sqrt{p_x^2 + p_y^2}$ and the scattering angle ϕ is taken to be measured from a direction in the $x-y$ plane. Our code has the Cartesian coordinate system oriented such that this plane is parallel to the disk plane, and the z-axis is along the upward vertical direction.

The outgoing photon's polarization vector $\mathbf{p}'$ is in the plane containing $\mathbf{p}$ and $\mathbf{n}'$. Thus,

$$\mathbf{p}' = \frac{(\mathbf{n}' \times \mathbf{p}) \times \mathbf{n}'}{|(\mathbf{n}' \times \mathbf{p}) \times \mathbf{n}'|} = \frac{1}{\sin\theta}(\mathbf{p} - \mathbf{n}'\cos\theta). \tag{2.9}$$

[2] Whitney(1991b; 1991a) has conducted Monte Carlo calculations of the polarization of a magnetized, electron-scattering atmosphere. Her calculations provide an interesting contrast to ours, because she included magnetic corrections to the scattering cross-section, but neglected Faraday rotation. Her results are of relevance to magnetic white dwarf and neutron star atmospheres. Our work has neglected magnetic effects on the scattering cross-section but has included Faraday rotation. This is much more relevant to optical and ultraviolet radiation emerging from AGN accretion discs, because the corrections to the scattering cross-section are negligible.

Between scatterings, the polarization vector gets rotated due to Faraday rotation. From equation (2.3), the Faraday rotation angle is given by $\chi = \mathbf{b} \cdot \mathbf{n} \tau_{\rm T} \delta/2$, where $\tau_{\rm T}$ is the Thomson scattering depth along the photon path length, $\mathbf{b} = \mathbf{B}/B$ is a unit vector along the magnetic field, and

$$\delta \equiv \frac{3\omega_B c}{2\omega^2 r_0} \simeq 0.198 \left(\frac{\lambda}{5000\text{Å}}\right)^2 \left(\frac{B}{1\text{G}}\right). \tag{2.10}$$

Thus, the photon polarization vector after rotation becomes

$$\mathbf{p}_{\rm rot} = \mathbf{p} \cos\chi + (\mathbf{n} \times \mathbf{p}) \sin\chi. \tag{2.11}$$

In the case of zero magnetic field, symmetry considerations imply that the polarization is linear and can have only two orientations for a given line of sight: parallel to the plane of the disk or in a plane perpendicular to the disk. Faraday rotation by a uniform magnetic field breaks this symmetry. The polarization will still be linear[3], but the plane of polarization can be at an arbitrary angle to the disk. Upon emerging from the atmosphere, we put the jth photon in an angle bin, and project its polarization vector onto two axes, one parallel to the plane of the disk and one perpendicular to this axis. The corresponding components are given by p_{0_j} and p_{90_j}, respectively. We then calculate the Stokes parameters, Q_j and U_j, for this photon from

$$Q_j = p_{0_j}^2 - p_{90_j}^2 \text{ and } U_j = 2 p_{0_j} p_{90_j}. \tag{2.12}$$

(The definition for U is equivalent to $U_j = p_{45_j}^2 - p_{135_j}^2$.) Finally, we sum Q_j and U_j over all the photons and divide by the number of photons in one angle bin to give the total Q/I and U/I for that viewing angle i. The Stokes parameter V vanishes because the polarization is linear. The degree of polarization is then calculated from $P = (Q^2 + U^2)^{1/2}/I$. The position angle of the polarization, measured counterclockwise (looking back along the line of sight towards the disk) from the axis which is parallel to the plane of the disk, is given by

$$\psi = (1/2) \tan^{-1}(U/Q), \tag{2.13}$$

with $0 \le \psi \le 90^\circ$ for $U \ge 0$ and $90^\circ \le \psi < 180^\circ$ for $U \le 0$.

[3]Magnetic corrections to the scattering cross section [cf. equation (2.4)] produce circular dichroism which would produce a small circular polarization (e.g. Silant'ev 1979).

2.2.2 Feautrier radiative transfer

One of the advantages of the Monte Carlo technique is that it is capable of handling general, complex geometries. However, it requires a very large number of photons to get accurate results, and is difficult to properly include thermal emissivity throughout the atmosphere. Thus, we derive here the radiative transfer equations including polarization restricted to plane-parallel atmospheres with a uniform, vertical magnetic field. The radiation field will then be completely axisymmetric and depend only on vertical depth. In this case it is straightforward to include the Faraday rotation directly in the full radiative transfer equation by just adding an extra term. This equation can then be solved much more quickly using standard numerical techniques.

The full polarized radiative transfer equation for a general magnetoactive plasma is already well-known (see e.g. Silant'ev 1979). However, because in our case it is so simple and illuminates the physics, we now briefly sketch a derivation of the Faraday rotation term.

We first project the photon polarization vector on two orthogonal axes which are perpendicular to the propagation direction $\mathbf{n}$. Let the first axis be parallel to the plane of the atmosphere, and the corresponding polarization vector component be p_0. Let the polarization vector component with respect to the second axis be p_{90}. Then equation (2.11) implies that after Faraday rotation,

$$p_{0\mathrm{rot}} = p_0 \cos\chi - p_{90} \sin\chi \tag{2.14}$$

and

$$p_{90\mathrm{rot}} = p_0 \sin\chi + p_{90} \cos\chi. \tag{2.15}$$

Following Chandrasekhar (1960), define $I_{r\nu}$ and $I_{l\nu}$ as the intensities of the radiation corresponding to p_0 and p_{90}, respectively. The Stokes parameter Q_ν may then be defined as $I_{r\nu} - I_{l\nu}$. In a similar fashion, let U_ν be the Stokes parameter with respect to two axes rotated by 45 degrees from those defined previously. The Stokes parameter V_ν vanishes because the radiation is linearly polarized. Expressed in terms of the total specific intensity $I_\nu = I_{r\nu} + I_{l\nu}$ and averaged over the individual polarization vectors of the corresponding photons, we have $Q_\nu = I_\nu(< p_0^2 > - < p_{90}^2 >)$ and $U_\nu = I_\nu < 2p_0 p_{90} >$. The degree of polarization is

$$P = \frac{(Q_\nu^2 + U_\nu^2)^{1/2}}{I_\nu}. \tag{2.16}$$

We now describe the intensity and polarization of the radiation field with the column vector

$$\mathbf{I}_\nu(\tau_\nu, \mu) = \begin{pmatrix} I_\nu \\ Q_\nu \\ U_\nu \end{pmatrix}. \tag{2.17}$$

From equations (2.14) and (2.15), Faraday rotation transforms the radiation field according to

$$\mathbf{I}_{\nu\mathrm{rot}} = \begin{pmatrix} 1 & 0 & 0 \\ 0 & \cos 2\chi & -\sin 2\chi \\ 0 & \sin 2\chi & \cos 2\chi \end{pmatrix} \mathbf{I}_\nu. \tag{2.18}$$

Let z be the height measured vertically upward in the atmosphere. Then for an infinitesimal change in height dz, the corresponding Faraday rotation angle for a vertical magnetic field is

$$d\chi = \mp\frac{1}{2}\delta n_e \sigma_T dz, \tag{2.19}$$

where the upper (lower) sign is to be taken for an upward (downward) directed field. Expanding equation (2.18), we deduce that the effect of Faraday rotation by a vertical magnetic field can be described by

$$\frac{\partial \mathbf{I}_\nu}{\partial z} = n_e \sigma_T \mathbf{F} \mathbf{I}_\nu, \tag{2.20}$$

where

$$\mathbf{F} \equiv \pm\delta \begin{pmatrix} 0 & 0 & 0 \\ 0 & 0 & 1 \\ 0 & -1 & 0 \end{pmatrix}. \tag{2.21}$$

Note that $\mathbf{F}$ does not change the total intensity, as expected.

Inserting this term into the full radiative transfer equation, we have

$$\begin{aligned} \mu\frac{\partial \mathbf{I}_\nu}{\partial z} &= \eta_\nu \begin{pmatrix} 1 \\ 0 \\ 0 \end{pmatrix} - (\kappa_\nu + n_e\sigma_T)\mathbf{I}_\nu + \mu n_e \sigma_T \mathbf{F}\mathbf{I}_\nu \\ &\quad + \frac{3}{8} n_e \sigma_T \int_{-1}^{1} d\mu' \mathbf{P}(\mu, \mu')\mathbf{I}_\nu(\mu'), \end{aligned} \tag{2.22}$$

where η_ν is the thermal emission coefficient (assumed unpolarized),

$$\mathbf{P}(\mu, \mu') \equiv \begin{pmatrix} \frac{4}{3}\left[1 + \frac{1}{2}P_2(\mu)P_2(\mu')\right] & (1-\mu'^2)P_2(\mu) & 0 \\ (1-\mu^2)P_2(\mu') & \frac{3}{2}(1-\mu^2)(1-\mu'^2) & 0 \\ 0 & 0 & 0 \end{pmatrix}, \tag{2.23}$$

and $P_2(\mu) \equiv (3\mu^2 - 1)/2$ is a second order Legendre polynomial (Chandrasekhar 1960; Loskutov and Sobolev 1979). Switching to the total optical depth τ_ν as the dependent variable in the usual way,

$$\begin{aligned} \mu \frac{\partial \mathbf{I}_\nu}{\partial \tau_\nu} &= \mathbf{I}_\nu - S_\nu(1-q_\nu) \begin{pmatrix} 1 \\ 0 \\ 0 \end{pmatrix} - \mu q_\nu \mathbf{F} \mathbf{I}_\nu \\ &\quad - \frac{3}{8} q_\nu \int_{-1}^{1} d\mu' \mathbf{P}(\mu, \mu') \mathbf{I}_\nu(\mu'), \end{aligned} \tag{2.24}$$

where $S_\nu \equiv \eta_\nu / \kappa_\nu$ is the thermal source function.

The formal solution for equation (2.24) can be expressed in terms of the total source function:

$$\mathfrak{S} \equiv \begin{pmatrix} \Im_I \\ \Im_Q \\ \Im_U \end{pmatrix} \equiv S(1-q) \begin{pmatrix} 1 \\ 0 \\ 0 \end{pmatrix} + \frac{3}{8} q \int_{-1}^{1} d\mu' \mathbf{P}(\mu, \mu') \mathbf{I}(\mu'). \tag{2.25}$$

(Note that $\Im_U = 0$ and $\Im_Q$ only has a contribution from scattering.) Then, the formal solution is given by:

$$\mathbf{I}(0, \mu) = \int_0^\infty \begin{pmatrix} 1 & 0 & 0 \\ 0 & \cos t\delta q & \pm \sin t\delta q \\ 0 & \mp \sin t\delta q & \cos t\delta q \end{pmatrix} \mathfrak{S}(t, \mu) e^{-t/\mu} \frac{dt}{\mu}, \tag{2.26}$$

where the sign convention is the same as for equation (2.19). The matrix represents the effect of Faraday rotation from the point of emission or last scattering to the top of the atmosphere (cf. eq. 2.18).

We have applied the Feautrier technique (e.g. Mihalas and Mihalas 1984; Phillips and Mészáros 1986) to solving equation (2.24) subject to the boundary condition that there be no external illumination of the atmosphere at $\tau_\nu = 0$. Unless otherwise noted, we calculate the integrals over μ with sixteen point Gaussian quadratures and use a logarithmically spaced grid in τ. For this chapter, we assume $\kappa_\nu = 0$ (i.e. $q = 1$) and $\eta_\nu = 0$; however, in chapter 4 we will include the effects of absorption and thermal emission.

2.3 Results

2.3.1 Constant vertical magnetic field: Monte Carlo results

The Stokes parameters for a uniform magnetic field, directed vertically upwards through the disk atmosphere, are presented in figures 2.3.1 and 2.3. The number of photons used in the Monte Carlo simulations for each value of δ was 10^8. We considered only optically thick atmospheres, and chose a vertical Thomson depth of $\tau_{\rm T} = 6$ from the lower (reflecting) boundary to the surface. Calculations with larger $\tau_{\rm T}$ did not produce significantly different results. The photons were binned into 100 equally spaced values of $\mu \equiv \cos i$. Our results agree very well with Chandrasekhar (1960) in the limit of zero magnetic field ($\delta \to 0$).

We have found that the Monte Carlo results can be approximately fit with a function of the form

$$Q(\mu,\delta)/I = Q_\circ \frac{e^{-a\mu} + e^{-b\mu} - e^{-a} - e^{-b}}{2 - e^{-a} - e^{-b}}, \tag{2.27}$$

where $Q_\circ = 0.11713$, $a = (0.573\delta + 0.876)$, and $b = (1.61\delta + 5.86)$; and

$$U(\mu,\delta)/I = U_\circ (1 - e^{-c\delta\mu}) \left(\frac{1}{d + \delta\mu^f} - \frac{1}{d+\delta} \right), \tag{2.28}$$

where $U_\circ = 0.08689$, $c = 2.95$, $d = 1.64$, and $f = 1.10$. These fitting functions are illustrated in figure 2.3.1 as well. The average deviation of the Monte Carlo points from the fit is 0.0024 for Q/I and 0.001 for U/I. The polarizations resulting from these fits are shown in figure 2.3. The total limb darkening is the same as in the case with no magnetic field.

One can estimate the depolarization due to a vertical magnetic field by assuming that the polarization is the same as that for no magnetic field, and then calculating the Faraday rotation after last scattering. The probability that a photon that has emerged from the atmosphere came from an optical depth $\tau_{\rm T}$ back along the photon trajectory is $e^{-\tau_{\rm T}}$. Hence Faraday rotation after last scattering will give Stokes parameters

$$Q/I = \int_0^\infty P_{\rm C}(\mu) \cos(\mu\delta\tau_{\rm T}) e^{-\tau_{\rm T}}\, d\tau_{\rm T} \tag{2.29}$$

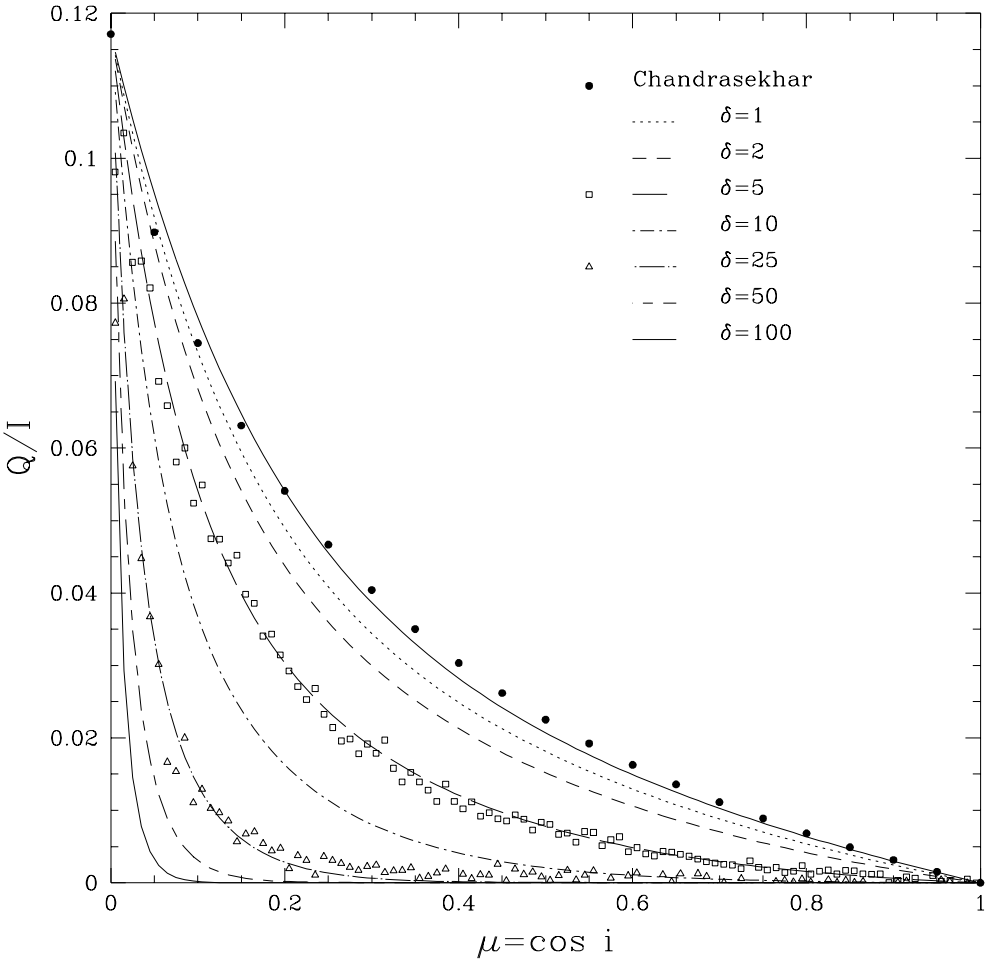

Figure 2.1: (a) Q/I for radiation emerging from a scattering atmosphere with a constant vertical magnetic field. The solid points are the exact data for the unmagnetized case from Chandrasekhar (1960). The lines are best fit curves to our Monte Carlo data (eqs. 2.27 and 2.28) for increasing values of δ. Two examples of the actual data from our Monte Carlo runs are also shown.

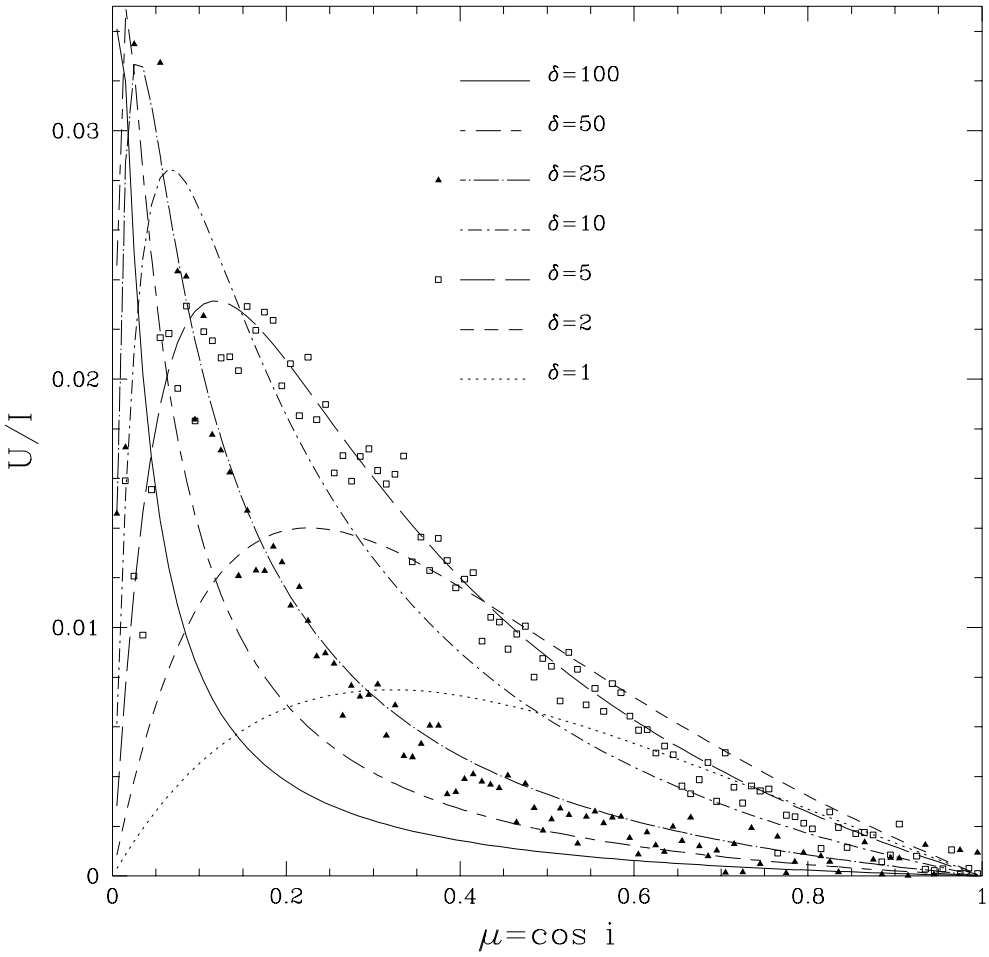

Figure 2.2: Same as figure 2.3.1, but for U/I.

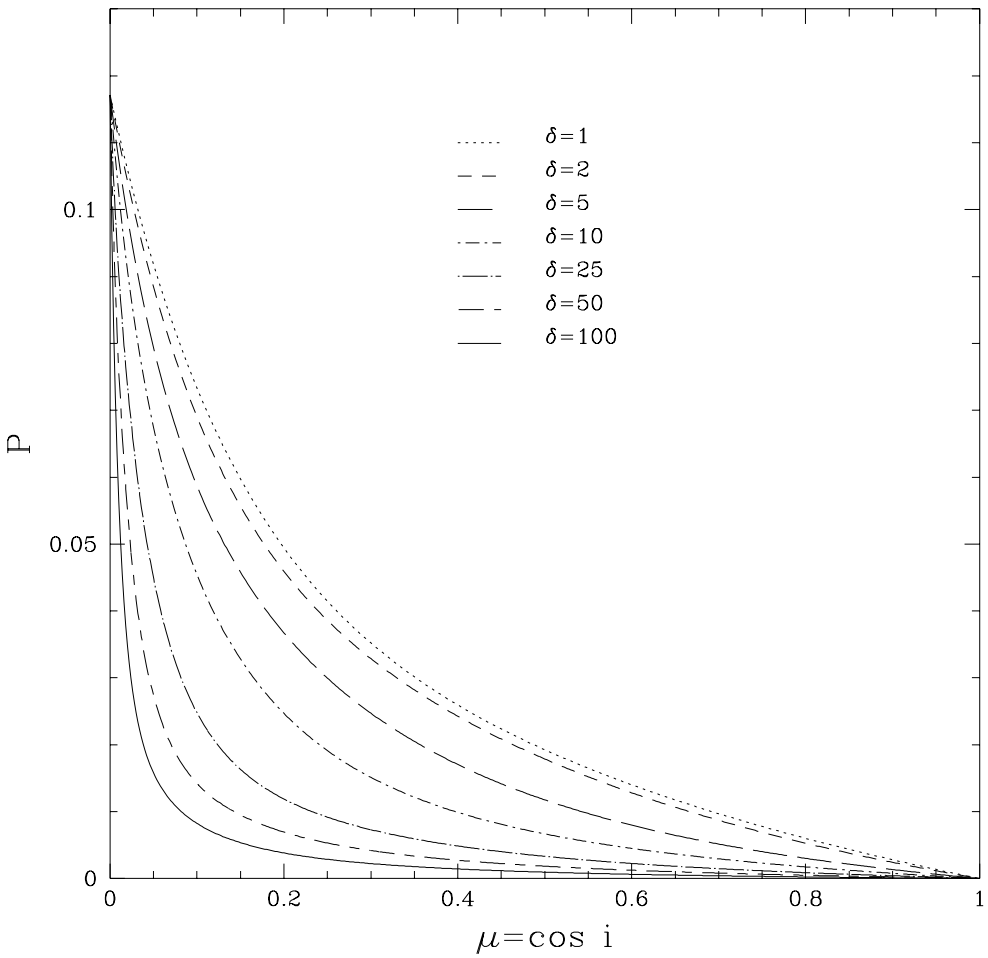

Figure 2.3: Degree of polarization for a vertical magnetic field, according to equations (2.27) and (2.28).

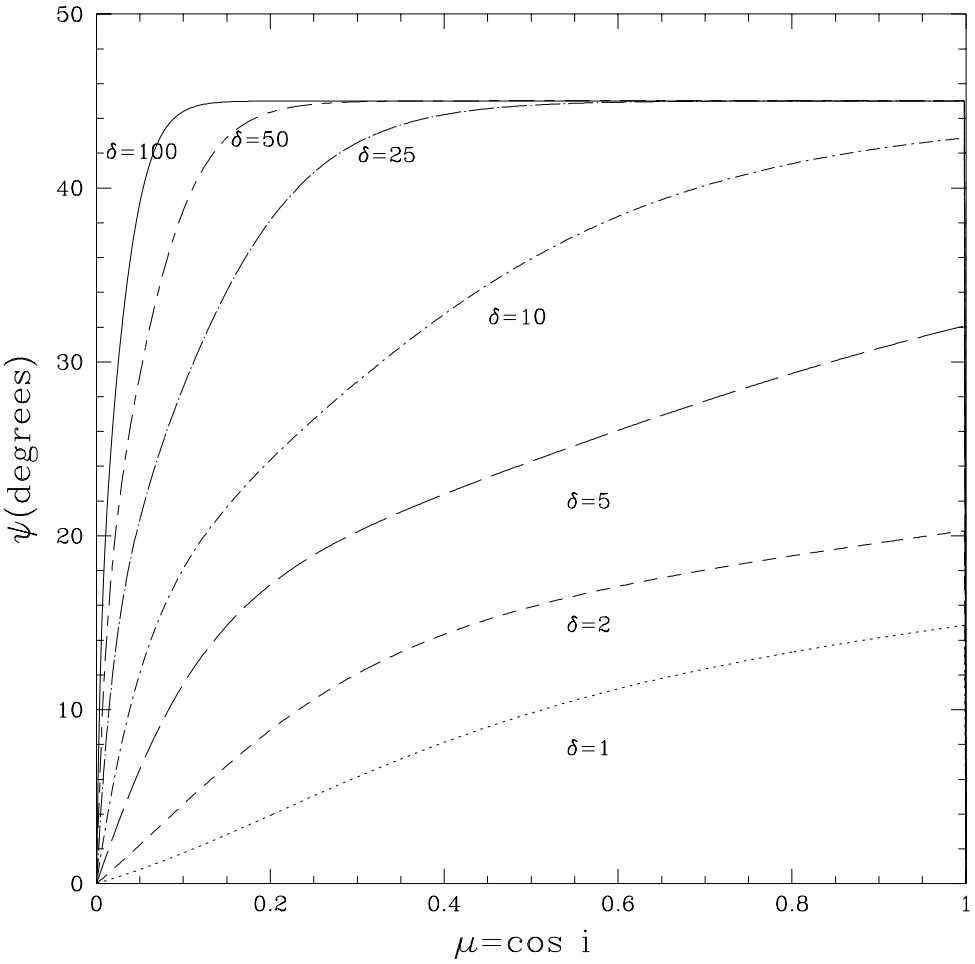

Figure 2.4: Same as figure 2.3, but position angle of polarization.

and

$$U/I = \int_0^\infty P_{\rm C}(\mu) \sin(\mu\delta\tau_{\rm T}) e^{-\tau_{\rm T}}\, d\tau_{\rm T}, \tag{2.30}$$

where $P_{\rm C}(\mu)$ is the polarization without magnetic field (Chandrasekhar 1960). We therefore find that

$$Q/I = \frac{P_{\rm C}(\mu)}{1+\delta^2\mu^2} \tag{2.31}$$

and

$$U/I = \frac{P_{\rm C}(\mu)\delta\mu}{1+\delta^2\mu^2}, \tag{2.32}$$

so

$$P = \frac{P_{\rm C}(\mu)}{(1+\delta^2\mu^2)^{1/2}}. \tag{2.33}$$

This shows qualitatively the correct behaviour, as it disagrees with our Monte Carlo simulations by less than 3% polarization, which indicates that Faraday rotation after last scattering is the most important effect. However, this estimate can fall fractionally below the simulations by as much as a factor of 65%, and thus is not accurate enough to calculate polarization expectations. The fact that Faraday rotation has its most important effect after last scattering explains why there is virtually no depolarization along lines of sight perpendicular to the vertical magnetic field ($\mu = 0$). This is consistent with the fact that the limb darkening does not vary significantly with δ.

2.3.2 Constant vertical magnetic field: finite difference results

We have calculated the polarization as described in section 2.2.2 for a variety of magnetic fields, and found very good agreement with the Monte Carlo results. Our results may be compared to those of Silant'ev (1979), who considered the polarization of radiation emerging from a plane parallel, optically thick scattering atmosphere with a uniform vertical magnetic field, and found

$$P = 0.0914\frac{(1-\mu^2)\varphi(\mu)}{H(\mu)(1+\delta^2\mu^2)^{1/2}}. \tag{2.34}$$

The functions $\varphi(\mu)$ and $H(\mu)$ are defined in the appendix (equations 2.58 and 2.64) and approach unity as $\mu \to 0$. Equation (2.34) was derived under the

assumption that $\delta \to \infty$, rejecting terms of order $\delta^{-1} \ln \delta$ in the coupled radiative transfer equations. The dependence of P on δ in equation (2.34) is identical to the crude approximation that Faraday rotation only takes place after last scattering [equation (2.33) above], and this is also true of Silant'ev's expressions for Q/I and U/I. We obtain good agreement with equation (2.34) in the limit of high δ away from $\mu = 0$. However, for low magnetic fields, where Silant'ev's approximation is of course not valid, equation (2.34) does not agree well with our Monte Carlo results. For reference, we rederive equation (2.34) in the appendix, section 2.6, using our notation.

Figure 2.5 shows a comparison of our numerical results with the high δ calculation of Silant'ev (1979). It is quite challenging to calculate the high δ case numerically. Finely spaced grid points are necessary to capture the rapid rotation of the polarization angle with depth. For $\delta = 50$, we reached convergence only with 20,000 logarithmically spaced depth points from $\tau = 10^{-5}$ to $\tau = 10$ for 8 angular points (a run with 4 angle points and 40,000 depth points agreed with this run). Even larger δ becomes numerically prohibitive because of the large number of matrices that need to be stored in the Feautrier method. In any case we find good agreement with Silant'ev's formula for large δ.

Since our Feautrier calculations are more accurate than the Monte Carlo calculations, we can assess the accuracy of the analytic fitting formulae found in section 2.3.1. For cases with $\delta \leq 10$, our fitting formulae are accurate to better than 12 per cent for P, 9 per cent for Q/I, and 35 per cent for U/I (it is least accurate when μ is very small). Silant'ev's formula can be used when $\delta \geq 10$, where it is accurate to better than 11 per cent for P.

If the disk has a uniform field that is not vertical, the axisymmetry is broken. As we have demonstrated, most of the depolarization comes from the last scattering in which photons scattered from different optical depths get rotated by different amounts by Faraday rotation. Since this is proportional to $\mathbf{n} \cdot \mathbf{B}$, we expect that the polarization for a given $\mathbf{n}$ and $\mathbf{B}$ should be approximately the same as in the vertical field case with μ still given by the angle of inclination from the vertical and B replaced by $\mathbf{n} \cdot \mathbf{B}$.

We have not run any optically thin simulations, but we expect that the Faraday depolarization would become less severe in such cases as $\tau_{\rm T}\delta$ becomes small.

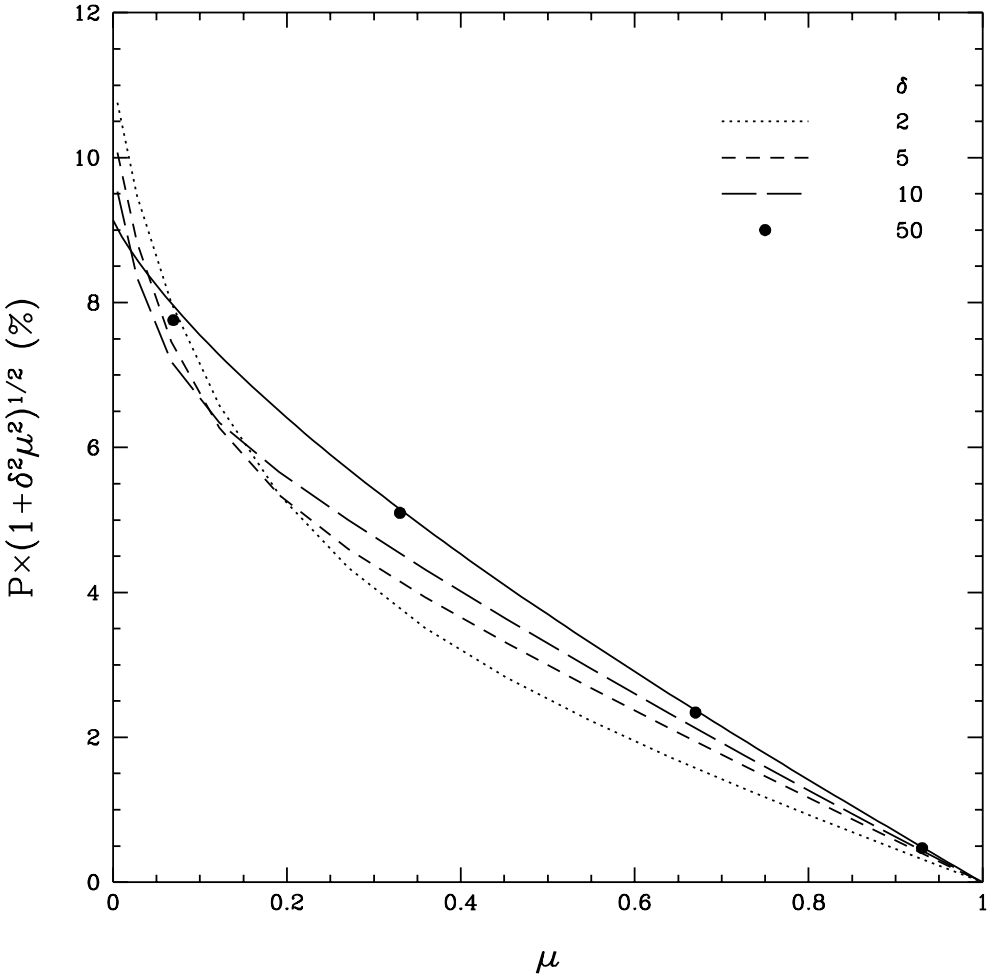

Figure 2.5: Polarization multiplied by $(1 + \mu^2\delta^2)^{1/2}$ for various δ's. The solid curve represents Silant'ev's formula 2.34 for large δ, while the dashed curves and points depict the results of our Feautrier code.

2.3.3 Random magnetic field: Monte Carlo results

Next, we consider a constant magnetic field with random orientation. This case cannot be handled in our Feautrier code since azimuthal symmetry is necessary in the current version of our code. For each photon, we chose a random direction for the magnetic field and propagated the photon out of the atmosphere with the same constant magnetic field. Since the symmetry is the same as for an atmosphere with no magnetic field, U is zero for all values of δ. We fit the Monte Carlo results for Q/I with the following function:

$$Q(\mu,\delta)/I = P_{\rm C}(\mu)R(\delta) = P_{\rm C}(\mu)\frac{1+a\delta}{1+a\delta+b\delta^2}, \tag{2.35}$$

where $a = 0.821$ and $b = 0.363$. The average error per point is 0.005. For $P_{\rm C}(\mu)$ we used the analytic fitting function from Bochkarev, Karitskaya, and Shakura (1985). Figure 2.6 compares this fit with the Monte Carlo data for Q/I. The polarization at $\mu = 0$ is decreased from the vertical field case since $\mathbf{n}\cdot\mathbf{B} \neq 0$ (there is now nonzero field in the plane of the disk).

We may again estimate the depolarization due to a random magnetic field by assuming that the polarization is the same as that for no magnetic field, and then calculating the Faraday rotation after last scattering. This gives

$$P = \frac{1}{2}\int_0^\infty\int_{-1}^{1} P_{\rm C}(\mu)\cos(\mu'\delta\tau_{\rm T})e^{-\tau_{\rm T}}\, d\mu'\, d\tau_{\rm T}, \tag{2.36}$$

where μ' is the angle between the magnetic field and the line of sight. Evaluating the integral,

$$P = \frac{P_{\rm C}(\mu)}{\delta}\tan^{-1}(\delta). \tag{2.37}$$

This shows qualitatively the correct behaviour, but falls below our Monte Carlo simulations by a factor of ~ 2 for larger δ.

2.4 Polarization of magnetized disks

The results obtained in the previous section can be used to model the polarized radiation emerging from an electron-scattering dominated accretion disk. We consider the inner regions of a geometrically thin and flat disk where the

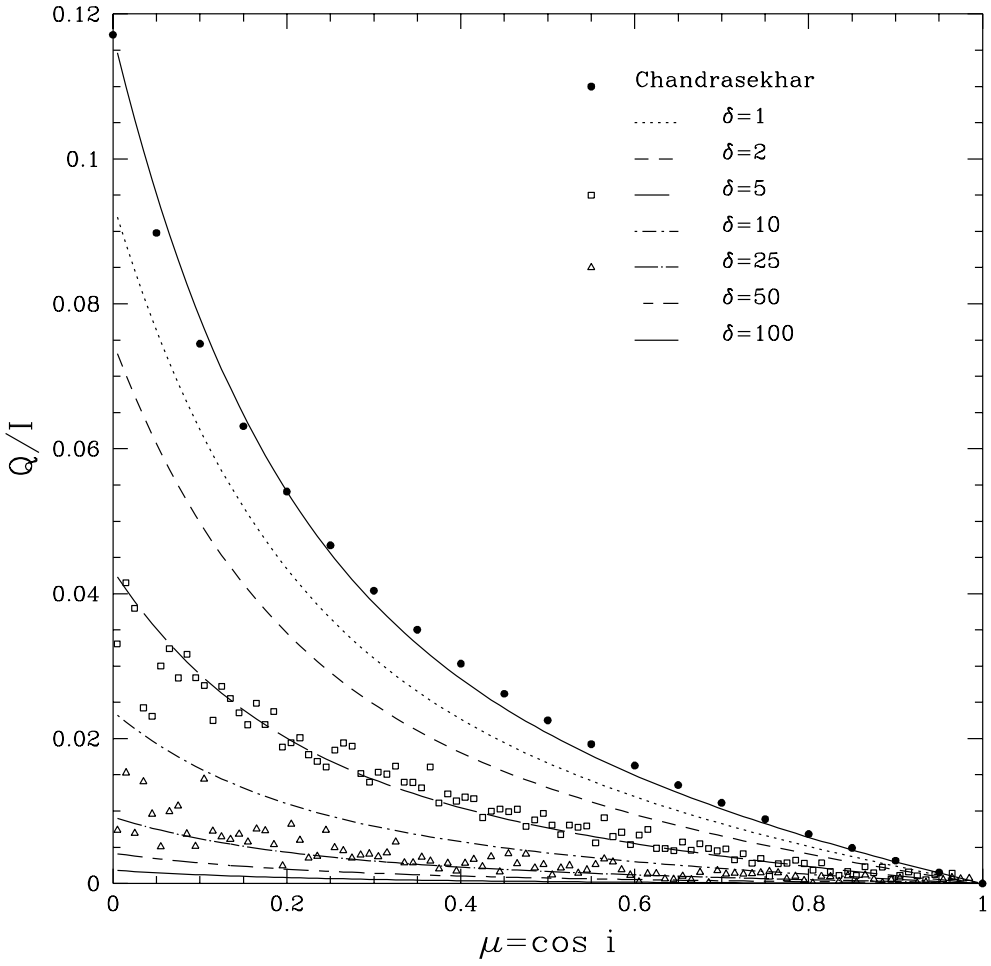

Figure 2.6: Q/I $(= P)$ for radiation emerging from a scattering atmosphere with a random magnetic field of constant strength. As in figure 2.3.1, the solid points are the exact data for the unmagnetized case from Chandrasekhar (1960). The lines are best fit curves to our Monte Carlo data [equation (2.35)] for increasing values of δ. Two examples of the actual data from our Monte Carlo runs are also shown.

atmosphere is optically thick to electron scattering. The constant (in magnitude) overall magnetic field strength assumed in the Monte Carlo simulations also requires us to make the reasonable assumption that locally the photons do not travel very far horizontally before escaping and the magnetic field does not change much in magnitude over several Thompson depths.

We need to specify the radial dependence of the field strength near the disk photosphere, $B(r)$. As discussed in section 2.1, our current understanding of magnetic fields in accretion disks cannot predict this, but it may be reasonable to assume that in the disk interior the field energy density is in equipartition with the thermal energy density. For a standard Novikov-Thorne disk, this gives

$$B \simeq 1 \times 10^5 \mathrm{G} \alpha^{-1/2} \left(\frac{M}{10^8 \ \mathrm{M}_\odot} \right)^{-1/2} \left(\frac{r}{r_\mathrm{g}} \right)^{-3/4} \mathcal{A}^{-1} \mathcal{B} \mathcal{E}^{1/2}. \tag{2.38}$$

If, on the other hand, we assume that such equipartition occurs just beneath the disk photosphere, we obtain

$$B \simeq 2 \times 10^5 \mathrm{G} \eta^{-1/2} \left(\frac{M}{10^8 \ \mathrm{M}_\odot} \right)^{-1/2} \left(\frac{\dot{M}}{\dot{M}_\mathrm{Edd}} \right)^{1/2} \left(\frac{r}{r_\mathrm{g}} \right)^{-3/2} \mathcal{Q}^{1/2} \mathcal{B}^{-1/2} \mathcal{C}^{-1/4}, \tag{2.39}$$

where $\dot{M}_\mathrm{Edd} \equiv L_{Edd}/\eta/c^2$ is the Eddington accretion rate and η is the efficiency appropriate for the angular momentum of the black hole. The quantities $\mathcal{A}$, $\mathcal{B}$, $\mathcal{C}$, $\mathcal{E}$, and $\mathcal{Q}$ are relativistic correction factors (Novikov and Thorne 1973; Page and Thorne 1974), all of which tend to unity at large radii. With the chosen scalings, the field strength in both equations (2.38) and (2.39) is about the same near the inner edge of the disk, but equipartition near the disk photosphere causes the field to decay more rapidly with radius. Given the large uncertainties, we have decided to assume that the field is in equipartition at the disk inner edge, and then parameterized the radial dependence of the field as a power law, i.e.

$$B = 1 \times 10^5 \mathrm{G} \alpha^{-1/2} \left(\frac{M}{10^8 \ \mathrm{M}_\odot} \right)^{-1/2} \left(\frac{r}{r_\mathrm{g}} \right)^{-\beta}. \tag{2.40}$$

Then, $\beta = 0.75$ corresponds to the case in which the magnetic field strength is independent of height in the disk, equation (2.1) above. Equipartition at the disk photosphere corresponds to $\beta = 1.5$. In addition, the self-similar outflow models of Blandford and Payne (1982) are described by a similar power law with $\beta = 1.25$.

We begin by neglecting Doppler shift, gravitational redshift, and aberration, both for simplicity and because it clarifies the effects of Faraday rotation alone. We also adopt the standard Shakura and Sunyaev (1973) α disk equations when describing the disk structure while we neglect these relativistic effects. We took a Schwarzschild black hole of mass 10^8 $M_\odot$ and a disk with $\dot{M} = 0.3\dot{M}_{\rm Edd}$, $\alpha = 0.1$, $\mu = 0.5$, and a field with random topology. We adopted a modified blackbody spectrum $f_\lambda(r)$ at each radius, and calculated it between 10 and 10000 Å, for disk radii from 6 to 10^3 gravitational radii. The temperature of the modified blackbody is given by (Novikov and Thorne 1973)

$$T_s = 1.3 \times 10^5 {\rm K} \left(\frac{F(r)}{10^{15} {\rm ergs\,cm^{-2}\,s^{-1}}} \right)^{4/9} \left(\frac{\rho(r)}{10^{-10} {\rm g\,cm^{-3}}} \right)^{-2/9}, \qquad (2.41)$$

where $F(r)$ is the flux at a given radius, $\rho(r)$ is the density at the midplane of the disk as a function of radius, numerically calculated from the disk structure equations assuming a one-zone model (the free-free gaunt factor was assumed to be unity). We assumed that the density at the midplane is the same as at the photosphere. Note that equation (2.41) neglects bound-free opacity, which is important in disks around massive black holes (e.g. Laor and Netzer 1989), and which we consider in the next chapter. We have also done calculations with a simple blackbody spectrum, and found very little difference in the resulting polarization.

The Stokes parameters for a given observer inclination angle are given by

$$\begin{pmatrix} I(\lambda) \\ Q(\lambda) \\ U(\lambda) \end{pmatrix} = \int_{r_{\rm i}}^{r_{\rm o}} 2\pi r dr \begin{pmatrix} 1 \\ Q(\mu,\delta)/I \\ U(\mu,\delta)/I \end{pmatrix} f_\lambda(r) \qquad (2.42)$$

where $r_{\rm i}$ and $r_{\rm o}$ are the inner and outer disk radii. $Q(\mu,\delta)/I$ and $U(\mu,\delta)/I$ are given by our fitting formulae to the Monte Carlo results, equations (2.27) and (2.28) above.

Figure 2.7 compares the polarization as a function of λ for values of β between 0.5 and 2. As expected, the polarization rises towards shorter wavelengths as Faraday rotation becomes less severe. At long wavelengths, when the polarization is low, the wavelength dependence obeys a power law, $P \propto \lambda^{-\gamma}$, where $\gamma = -2 + 0.75\beta$. For a constant magnetic field ($\beta = 0$), this agrees with the λ^{-2} dependence found by Gnedin and Silant'ev (1978). Figure 2.8 shows the results

for the polarization for various black hole masses. Faraday depolarization becomes increasingly important at short wavelengths and as the black hole mass decreases.

To examine the additional effects of Doppler shifts, gravitational redshift, aberration (usually described by a "relativistic transfer function"), and a more realistic disk spectrum, we put our results for the random magnetic field into the code used in LNP, which was kindly provided by Ari Laor. The polarization that they calculated used the Chandrasekar formula. To take into account absorption in the atmosphere, they simply multiplied $P_{\rm C}(\mu)$ by

$$q(\nu) = \frac{\kappa_{\rm es}}{\kappa_{\rm es} + \kappa_{\rm ab}(\nu)}, \tag{2.43}$$

where $\kappa_{\rm ab}$ and $\kappa_{\rm es}$ are the absorption and electron-scattering opacities, respectively. To include the effects of a magnetic field, we further multiplied by $R(\delta(B(r),\nu))$ from equation (2.35).[4] The radial dependence of B was again given by the power law (2.40). Note that all the relativistic corrections to the disk structure (Novikov and Thorne 1973; Page and Thorne 1974) are now again included. The results are presented in Figure 2.9 for a maximal Kerr disk model with $\alpha = 0.1$, $M_8 = 1$, $\dot{M} = 0.1\dot{M}_{\rm Edd}$, $\mu = 0.5$, $\beta = 0.75$, and viscous stress $t_{r\phi} = \alpha\sqrt{P_{\rm g}P_{\rm rad}}$ (see LNP for further details about their model). These approximations for the effects of magnetic field when absorption opacity is present are not very accurate; calculations of the disk atmosphere including absorption opacity and magnetic fields will be presented in chapters 3 and 4.

Five different cases were calculated which demonstrate the importance of different effects: (1) a disk without absorption and magnetic field, but with the transfer function; (2) a disk without absorption, but with the transfer function and magnetic field; (3) a disk without absorption and neglecting the transfer function, but with magnetic field; (4) a disk without magnetic field, but with absorption and the transfer function; and (5) a disk with absorption, magnetic field, and the transfer function. Cases (1) and (3) show that the effects of the transfer function are important in reducing the overall polarization at high frequencies, but the magnetic field plays a more important role at low frequencies. Cases (2) and (3) show that the transfer function enhances the Faraday depolarization in the frequency range of $10^{13} - 10^{18}$ Hz. As the disk becomes more

[4]It is fortunate that we found a good fit to the Monte Carlo data in this case that can be written as a product of $P_{\rm C}(\mu)$ with a function of δ alone. It is this fact that allows us to generalize their simple procedure.

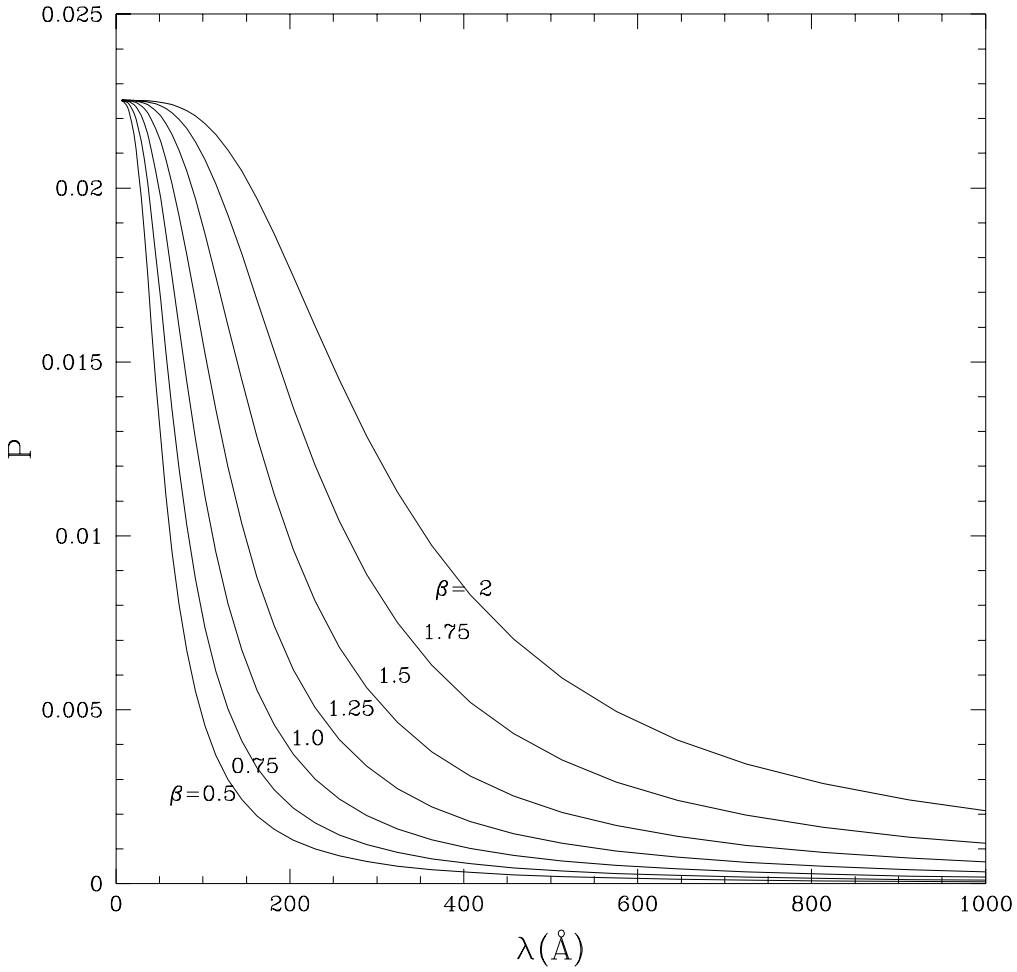

Figure 2.7: Wavelength dependence of polarization resulting from random magnetic fields with different radial power laws (eq. 2.40) in a Shakura-Sunyaev disk. The adopted parameters are $\alpha = 0.1$, $\mu = 0.5$, $M = 10^8$ $\mathrm{M}_\odot$, and $\dot{M} = 0.3\dot{M}_{\mathrm{Edd}}$.

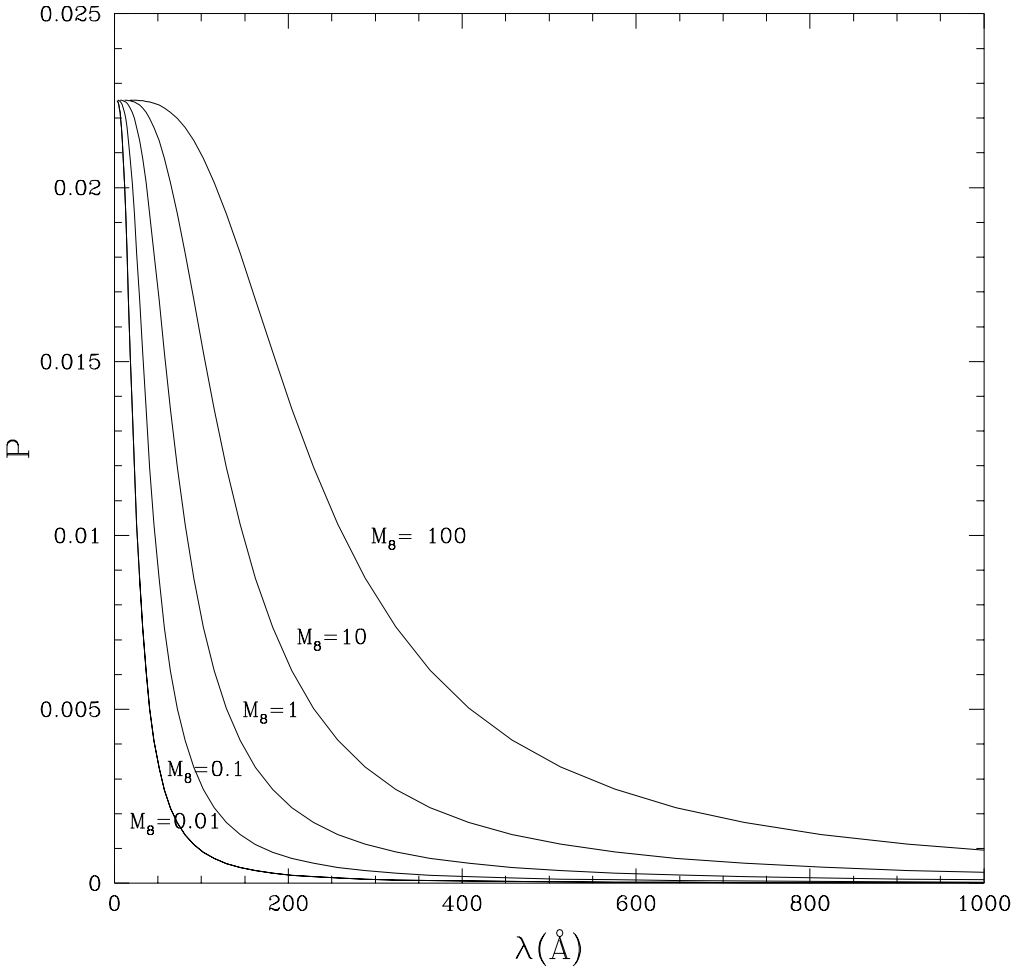

Figure 2.8: Wavelength dependence of polarization for random magnetic fields in a Shakura-Sunyaev disk with different black hole masses $M \equiv 10^8 M_8$ $\mathrm{M}_\odot$. The adopted parameters are $\alpha = 0.1$, $\mu = 0.5$, $\dot{M} = 0.3\dot{M}_{\rm Edd}$, and $\beta = 0.75$.

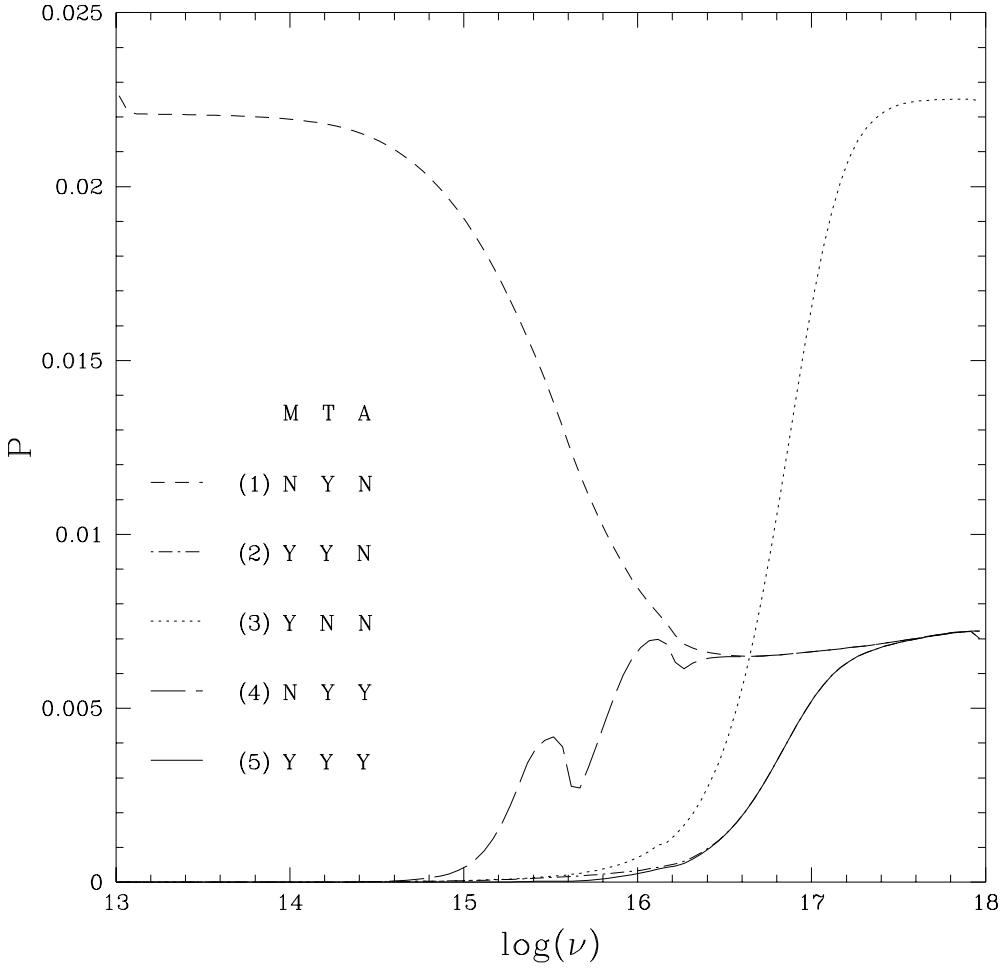

Figure 2.9: Wavelength dependence of polarization for relativistic disks around a maximally rotating Kerr hole. Cases with and without magnetic fields (M), the relativistic transfer function (T), and absorption opacity (A) are shown and described further in the text. The adopted parameters are $\alpha = 0.1$, $M = 10^8$ M$_\odot$, $\dot{M} = 0.1\dot{M}_{\rm Edd}$, $\mu = 0.5$, and $\beta = 0.75$.

face on, the difference between the cases with and without the transfer function decreases. Cases (2) and (4) show that Faraday rotation as we have treated it here can be much more important in reducing polarization than absorption (but see below). When we reduce the magnetic field to 1/10 of equipartition, then absorption and Faraday depolarization have comparable effects. Case (5) shows the complete effects of Doppler shifts, gravitational redshift, aberration, magnetic field, and absorption. As shown in figure 2.10, the same results hold for $\beta = 1.5$, except that the cases with magnetic field are shifted towards lower frequency from the $\beta = 0.75$ case.

We stress that all the calculations in this section are based on the results of our Monte Carlo simulations for a random magnetic field which completely neglected the effects of absorption opacity. If absorption opacity dominates over electron-scattering opacity, then the electron-scattering column down to unit optical depth would be reduced and therefore Faraday rotation would probably also be reduced in proportion to $q\tau_T\delta$. If absorption opacity plays a dominant role in determining the optical/UV radiation field of quasars, it is necessary to incorporate it directly in the computation of Faraday rotation before we can fully determine the effects of magnetic fields on polarization, which we do for vertical magnetic fields chapter 4.

2.5 Conclusions

The most important results of this work are the first fully self-consistent calculations of the effects of Faraday rotation on the polarization from plane-parallel, electron-scattering atmospheres. Equations (2.27), (2.28), and (2.35) provide accurate fitting formulae to our results which may be incorporated into electron-scattering dominated accretion disk models. In section 2.4 we presented examples of such disk models, and found that in the optical/UV waveband for AGN, Faraday rotation may play a dominant role in reducing the polarization.

A major uncertainty is the overall magnetic field strength, its topology, and its variation with disk radius and height. Numerical simulations will probably be necessary to obtain a better understanding of this. Sakimoto and Coroniti (1981) have argued that buoyancy will limit the magnetic field energy density in the disk interior to be less than the gas pressure, not the total pressure, since the photons will diffuse across a flux tube, equalizing the radiation pressure across the tube. In this case, the field strength could be much smaller than

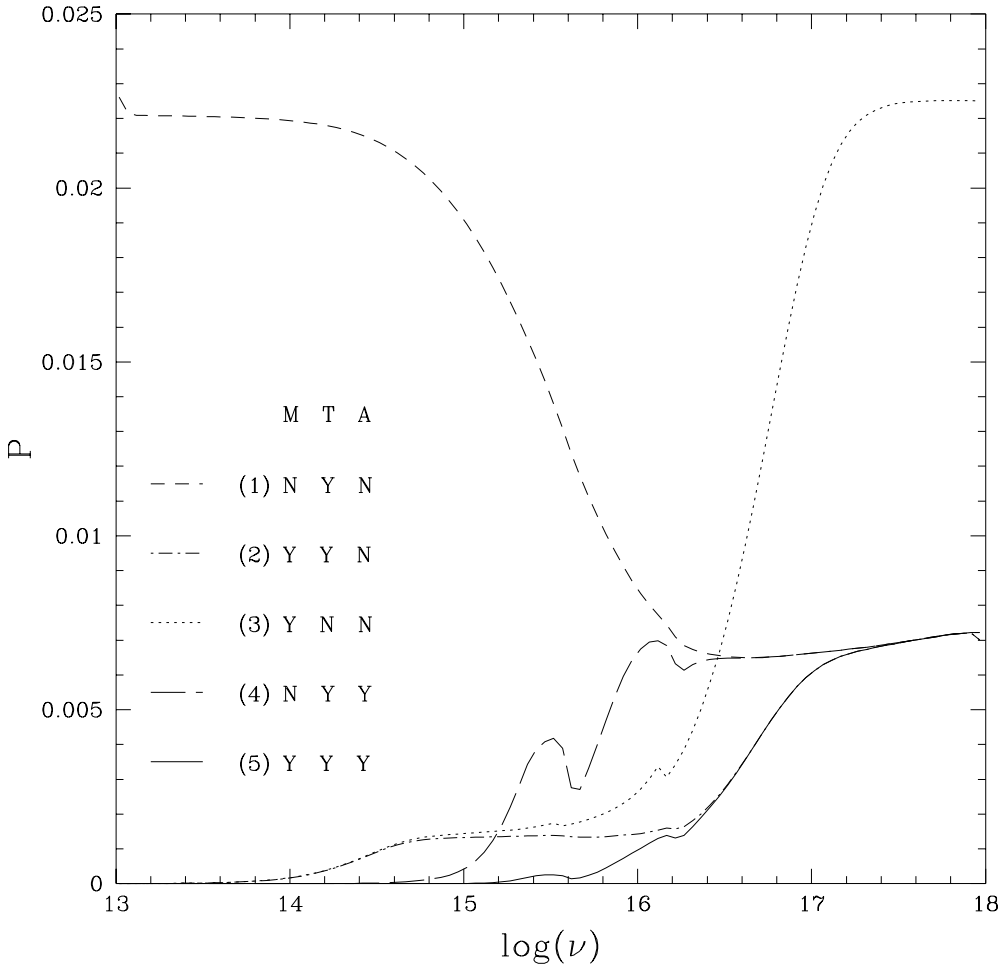

Figure 2.10: Same as figure 2.9 but for $\beta = 1.5$.

we have assumed in the inner, radiation-pressure supported regions of the disk. The recent simulations of Stone, Hawley, Gammie, and Balbus (1996) indicate, however, that buoyancy may not be an important factor in determining the field strength, as rapid local field generation causes the magnetic field to build up to super-equipartition strengths. We note that our calculations have assumed that the magnetic field lines have a covering factor of unity at the disk photosphere. If the covering fraction of magnetic field, f, is less than unity, then $P \simeq P_c(\mu)(1-f) + fP'(\mu)$, where P' is the polarization for an $f = 1$ disk model. It is possible that the field is concentrated in small structures with a low covering factor, as in our Sun or other G stars (Marcy 1984), in which case Faraday rotation would be diminished and the polarization would be increased.

It is unclear whether these results can actually help explain the polarization that is observed in AGN. The rise in polarization observed beyond the Lyman edge by Impey et al. (1995) and Koratkar et al. (1995) is far too steep to be explained by the simple Faraday rotation models we have considered here and occurs at longer wavelengths. However, a more gradual increase in polarization with frequency may be able to explain the rise in polarization that has been attributed to dust scattering (Webb et al. 1993). The polarization angle would still be expected to be perpendicular to the disk symmetry axis in AGN, at least for a random magnetic field. It is only possible to measure this axis in those AGN which have extended radio emission (assumed to be aligned along the symmetry axis). The polarization in these objects shows a clear tendency towards alignment (e.g. Stockman, Angel, and Miley 1979; Berriman et al. 1990). As shown by our analysis of the vertical field case, an ordered magnetic field could in principle produce a wavelength dependent rotation of the position angle as the polarization decreased, but this is unlikely to always produce a polarization along the disk symmetry axis.

At the 1994 spectropolarimetry conference at Caltech, Roger Blandford and Sterl Phinney suggested that the rise in polarization in 1630+377 could be due to a Faraday "screen" with the probability distribution of Faraday rotation parameter being a gaussian with zero mean and standard deviation σ_χ (corresponding to a magnetic field of strength σ_B). For example, if a magnetic field of strength B_o is distributed randomly in direction on a scale $L_B \ll L_{Th}$, which is the Thomson scattering length, then the average Faraday rotation parameter for a photon will be zero, with a standard deviation $\sigma_\chi \simeq \chi_o\sqrt{L_B/L_{Th}}$, where χ_o is the Faraday rotation parameter for field of strength B_o. Thus,

$\sigma_B/B_o = \sqrt{L_B/L_{Th}} \ll 1$. If the radiation is assumed to have polarization P_0 before passing through the screen, then the final polarization will be

$$P = P_0 e^{-(\lambda/\lambda_0)^4} \text{ where } \lambda_0 = 632\text{Å}\tau_{es}^{-1/2}(\sigma_B/2\times10^5 G)^{-1/4}, \tag{2.44}$$

where τ_{es} is the electron-scattering optical depth of the screen. In figure 2.11 we compare this model to the polarization of 1630+377 (Koratkar et al. 1995) assuming $P_0 = 100\%$ and $\lambda_0 = 610$Å (found using chi-by-eye). The solid lines are the observed flux, the observed flux times the Faraday screen polarization, and the Faraday screen polarization. The dashed line on the top panel shows the total flux minus the polarized flux shown in the middle panel. If $\tau_{es} = 1$, this λ_0 corresponds to $\sigma_B = 2\times10^5$ Gauss, roughly equipartition for the inner parts of an accretion disk (cf. equation 2.1). However, if this is due to a randomly distributed field of strength B_o as argued above, then $B_o \gg \sigma_B$. The magnetic field can be reduced if τ_{es} is larger; however, then the radiation will be scattered out of the line of sight. The fit looks rather good, and is essentially only one free parameter. It could be easily ruled out if the polarization is seen to drop at shorter wavelengths, since the model predicts it should continue to rise to 100% at $\lambda = 0$. One problem with this model is that it does not explain the polarization of the Lyman α line, which is larger than the continuum around it and has the same position angle as the polarization below the Lyman edge, and therefore one must invoke another model to explain why Lyman α is polarized at the same angle as the flux below the Lyman edge. Another problem is how to get 100% polarization of the radiation before it passes through the Faraday screen (this is even harder than getting the 20% observed polarization). It is also remarkable that the polarization rise seems to be associated with the Lyman edge, which requires a fine-tuned magnetic field dispersion to explain. If the starting polarization is lower, then the fit is poorer. Synchrotron emission is highly polarized, but to get 100% polarization would require a very ordered magnetic field viewed edge-on, in addition to anisotropic particle velocities. Scattering through 90° can cause 100% polarization, but again this requires a very special geometry (obscuration or beaming of the source, and a small solid angle in which the scattering occurs, giving a low flux). Either possibility might be realized in a jet scenario; however, the jet must be very compact to avoid reduction of the magnetic field as the plasma expands.

The results shown in figure 2.8 suggest that Faraday rotation is more important for lower mass black holes, so we would expect simple accretion disk models of AGN to produce higher optical/UV polarization in quasars than in Seyfert

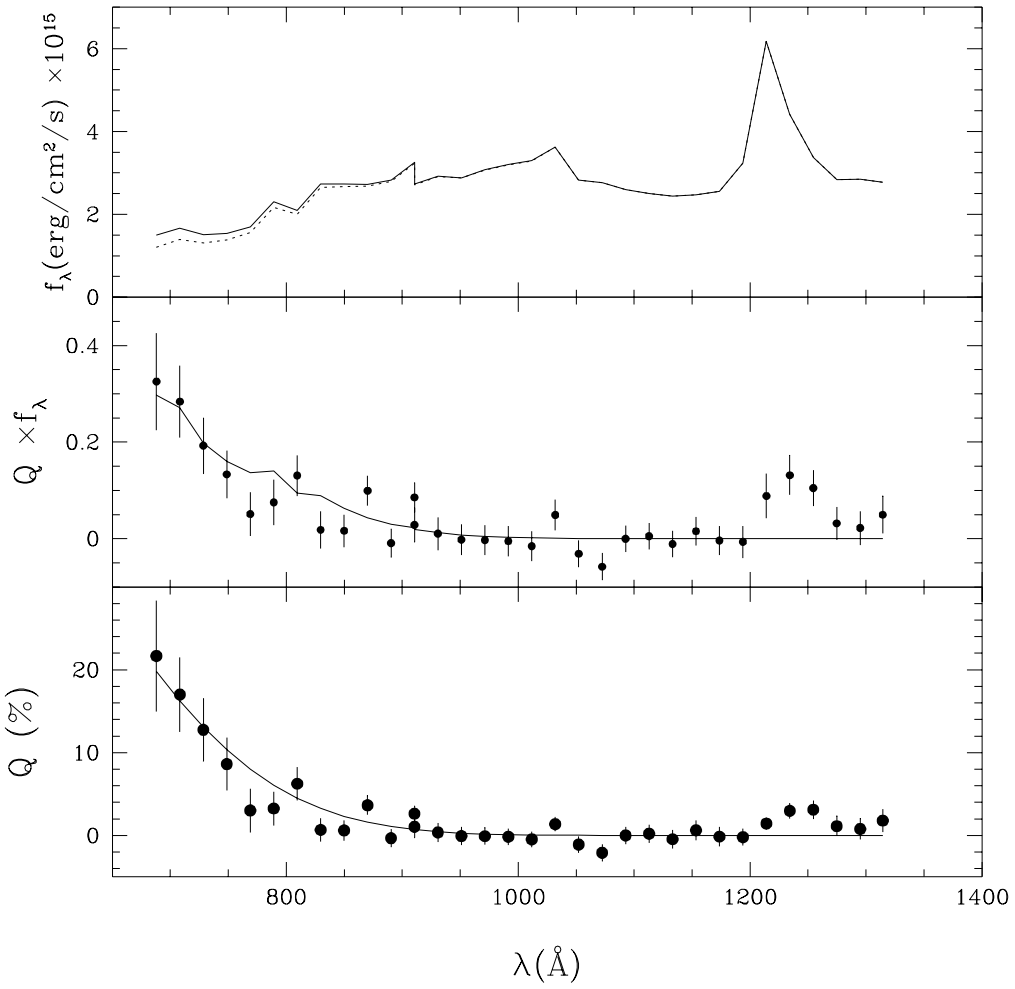

Figure 2.11: Flux, polarized flux, and polarization of 1630+377 (data courtesy of Bob Goodrich) compared with the polarization assuming the light is 100% polarized to begin with, but passes through a Faraday screen with $\tau_{es} = 1$, $\sigma_B = 2.3 \times 10^5 G$. The dashed line in the top panel is the flux minus the polarized flux.

1's. Our results may also be applied to stellar mass black holes. Equation (2.1) implies that for a ten solar mass Schwarzschild black hole, the Faraday rotation angle would exceed one radian for photons with energies as high as 7.6 keV near the inner edges of disks with $\alpha \sim 1$. Hence Faraday rotation may also play a significant role in the polarization signature of black hole candidate X-ray binaries, as was pointed out by Gnedin and Silant'ev (1977).

Chapter 4 will consider the effect of Faraday rotation in the presence of absorption opacity more accurately.

2.6 Appendix

We reproduce here Silant'ev's (1979) analytic calculation of the polarization of radiation emerging from an optically thick, pure electron scattering atmosphere in the $\delta \to \infty$ limit.

Silant'ev's calculation uses a radiation density matrix formalism, which is applicable to magnetic fields with arbitrary orientation. For a vertical magnetic field, however, it is somewhat simpler to use the radiative transfer equation as we have formulated it in section 2. We therefore proceed to show how Silant'ev's result can be derived within this formalism.

Define a complex intensity column vector

$$\mathbf{I}' = \begin{pmatrix} I/2^{1/2} \\ (-Q+iU)/2 \\ (-Q-iU)/2 \end{pmatrix}. \tag{2.45}$$

Then, for $q = 1$, the equation of transfer (2.24) may be written

$$\mu \frac{\partial \mathbf{I}'}{\partial \tau} = \mathbf{M}\mathbf{I}' - \frac{1}{2}\int_{-1}^{1} d\mu' \mathbf{P}'(\mu,\mu')\mathbf{I}'(\mu'), \tag{2.46}$$

where

$$\mathbf{M} = \begin{pmatrix} 1 & 0 & 0 \\ 0 & 1 \mp i\delta\mu & 0 \\ 0 & 0 & 1 \pm i\delta\mu \end{pmatrix}, \tag{2.47}$$

$$P'_{ij}(\mu,\mu') = a_i(\mu)a_j(\mu') + \delta_{i1}\delta_{j1}, \tag{2.48}$$

and

$$\mathbf{a}(\mu) = \left(-P_2(\mu)/2^{1/2}, 3(1-\mu^2)/4, 3(1-\mu^2)/4\right). \tag{2.49}$$

As in section 2.2, the upper and lower signs in equation (2.47) refer to upward and downward magnetic field directions, respectively. We have again suppressed the frequency subscript because there is no frequency redistribution in this problem.

Using a principle of invariance for vectors (cf. chapter 4 in Chandrasekhar 1960), the radiation field emerging from the atmosphere ($0 \le \mu \le 1$) can be expressed in terms of a scattering matrix $\mathbf{S}$:

$$\mathbf{I}'(0,\mu) = \begin{pmatrix} 1 & 0 & 0 \\ 0 & \frac{1}{1\mp i\delta\mu} & 0 \\ 0 & 0 & \frac{1}{1\pm i\delta\mu} \end{pmatrix} \left[\frac{1}{2}\int_0^1 \mathbf{P}'(\mu,\mu')\mathbf{I}'(0,\mu')d\mu'\right.$$

$$+\frac{1}{4}\int_0^1\int_0^1 \mathbf{S}(\mu,\mu')\mathbf{P}'(\mu',\mu'')\mathbf{I}'(0,\mu'')\frac{d\mu'}{\mu'}d\mu''\Bigg]. \tag{2.50}$$

The scattering matrix satisfies the following integral equation:

$$\begin{aligned}\left(\frac{1}{\mu}+\frac{1}{\mu_0}\right)\mathbf{S}(\mu,\mu_0) &\mp i\delta\mathbf{D}\mathbf{S}(\mu,\mu_0) \pm i\delta\mathbf{S}(\mu,\mu_0)\mathbf{D}\\ &= \mathbf{P}'(\mu,\mu_0)+\frac{1}{2}\int_0^1 \mathbf{P}'(\mu,\mu')\mathbf{S}(\mu',\mu_0)\frac{d\mu'}{\mu'}+\\ &\qquad \frac{1}{2}\int_0^1 \mathbf{S}(\mu,\mu')\mathbf{P}'(\mu',\mu_0)\frac{d\mu'}{\mu'}+\\ &\frac{1}{4}\int_0^1\int_0^1 \mathbf{S}(\mu,\mu')\mathbf{P}'(\mu',\mu'')\mathbf{S}(\mu'',\mu_0)\frac{d\mu'}{\mu'}\frac{d\mu''}{\mu''},\end{aligned} \tag{2.51}$$

where

$$\mathbf{D}=\begin{pmatrix}0&0&0\\0&1&0\\0&0&-1\end{pmatrix}. \tag{2.52}$$

Note that the symmetry of equations (2.48) and (2.51) implies that $\mathbf{S}(\mu,\mu_0)=\mathbf{S}(\mu_0,\mu)$.

Define

$$\boldsymbol{\gamma}(\mu,\mu_0)\equiv\mu+\mu_0\begin{pmatrix}1&1\pm i\delta\zeta&1\mp i\delta\zeta\\1\mp i\delta\zeta&1&1\mp 2i\delta\zeta\\1\pm i\delta\zeta&1\pm 2i\delta\zeta&1\end{pmatrix}, \tag{2.53}$$

(where $\zeta=\mu\mu_0/(\mu+\mu_0)$) and a matrix $\mathbf{T}(\mu,\mu_0)$ by letting

$$S_{ij}(\mu,\mu_0)\equiv\frac{\mu\mu_0}{\gamma_{ij}(\mu,\mu_0)}T_{ij}(\mu,\mu_0), \tag{2.54}$$

where no summation over the indices i and j is implied. In the limit of large δ, $1/\gamma_{ij}(\mu,\mu_0)=\delta_{ij}/(\mu+\mu_0)$, provided both μ and μ_0 are nonzero. If we make the ansatz that all elements of the matrix $\mathbf{T}$ remain finite for all values of μ and μ_0, then in this limit equation (2.51) simplifies to

$$T_{ij}(\mu,\mu_0)=H_i(\mu)H_j(\mu_0)+K_i(\mu)K_j(\mu_0). \tag{2.55}$$

Here

$$H_i(\mu)=a_i(\mu)+\frac{\mu}{2}\int_0^1\frac{T_{ii}(\mu,\mu')a_i(\mu')}{\mu+\mu'}d\mu', \tag{2.56}$$

$$K_i(\mu) = \delta_{i1}\left[1 + \frac{\mu}{2}\int_0^1 \frac{T_{11}(\mu,\mu')}{\mu+\mu'}d\mu'\right], \tag{2.57}$$

and we are considering both μ and μ_0 to be nonzero. Since $a_2(\mu) = a_3(\mu)$, the equations for T_{22} and T_{33} are identical. Let $H_2(\mu) = H_3(\mu) \equiv \frac{3}{4}(1-\mu^2)\phi(\mu)$. Then $\phi(\mu)$ satisfies the nonlinear equation

$$\phi(\mu) = 1 + \frac{9\mu\phi(\mu)}{32}\int_0^1 \frac{\phi(\mu')(1-\mu'^2)^2}{\mu+\mu'}d\mu'. \tag{2.58}$$

The equation for T_{11} may be written

$$T_{11}(\mu,\mu_0) = \frac{3}{8}\left[\frac{1}{3}\psi(\mu)\psi(\mu_0) + \frac{8}{3}\tilde{\phi}(\mu)\tilde{\phi}(\mu_0)\right], \tag{2.59}$$

where

$$\psi(\mu) \equiv 3 - \mu^2 + \frac{\mu}{2}\int_0^1 \frac{T_{11}(\mu,\mu')(3-\mu^2)}{\mu+\mu'}d\mu' \tag{2.60}$$

and

$$\tilde{\phi}(\mu) \equiv \mu^2 + \frac{\mu}{2}\int_0^1 \frac{T_{11}(\mu,\mu')\mu'^2}{\mu+\mu'}d\mu'. \tag{2.61}$$

Apart from multiplicative factors, equation (2.59) is identical to the equation for the first term of the scattering function $S^{(0)}(\mu,\mu_0)$ in the problem of diffuse reflection from a scattering medium described by Rayleigh's phase function (cf. equation 6 in section 44 of Chandrasekhar 1960).

The scattering matrix elements in the limit of large δ are therefore given by

$$S_{11}(\mu,\mu_0) = \frac{3}{8}\frac{\mu\mu_0}{\mu+\mu_0}H(\mu)H(\mu_0)[3 - c(\mu+\mu_0) + \mu\mu_0] \tag{2.62}$$

$$\begin{aligned} S_{22}(\mu,\mu_0) &= S_{33}(\mu,\mu_0) \\ &= \frac{9}{16}\frac{\mu\mu_0}{\mu+\mu_0}(1-\mu^2)(1-\mu_0^2)\phi(\mu)\phi(\mu_0) \end{aligned} \tag{2.63}$$

where $H(\mu)$ satisfies the integral equation,

$$H(\mu) = 1 + \frac{3}{16}\mu H(\mu)\int_0^1 \frac{(3-\mu'^2)}{\mu+\mu'}H(\mu')d\mu', \tag{2.64}$$

and

$$c \equiv \frac{\int_0^1 H(\mu)\mu^2 d\mu}{\int_0^1 H(\mu)\mu d\mu}. \tag{2.65}$$

The off-diagonal components of $\mathbf{S}(\mu, \mu_0)$ are negligible ($\sim \delta^{-1}$). Although these expressions were derived assuming both μ and μ_0 are nonzero, they remain valid even if this is not the case. This is because they then vanish provided $\mathbf{T}(\mu, \mu_0)$ is finite, which can easily be shown to be true.

Given this solution for $\mathbf{S}(\mu, \mu_0)$, we can calculate the outgoing radiation field from equation (2.50). We immediately conclude from the matrix multiplier in this equation that Q and U vanish as $\delta \to \infty$ for nonzero μ. The intensity is given by

$$I(0,\mu) = \frac{1}{2}\int_0^1 {P'}_{11}(\mu,\mu')I(0,\mu')d\mu' + \frac{1}{4}\int_0^1\int_0^1 S_{11}(\mu,\mu'){P'}_{11}(\mu',\mu'')I(0,\mu'')\frac{d\mu'}{\mu'}d\mu'', \tag{2.66}$$

which has solution

$$I(0,\mu) = \frac{FH(\mu)}{2\pi\int_0^1 \mu' H(\mu')d\mu'}, \tag{2.67}$$

where F is the flux emerging from the atmosphere. This is the same limb darkening law as that of radiation emerging from a scattering medium described by Rayleigh's phase function (cf. section 45 of Chandrasekhar 1960), i.e. an electron scattering medium in which the radiation is everywhere treated as unpolarized. This makes physical sense in the limit of infinite Faraday rotation, as Q and U approach zero.

Since the Q' and U' Stokes parameters are of minimum order δ^{-1} (for μ not equal to 0), we can ignore the contribution of Q' and U' in the integrals on the right hand side of equation (2.50). This then gives:

$$Q' = \frac{1}{1-i\delta\mu}\left[\frac{1}{2}\int_0^1 P'_{21}(\mu,\mu')I'(0,\mu')d\mu' + \frac{1}{4}\int_0^1\int_0^1 S_{22}(\mu,\mu')P'_{21}(\mu',\mu'')I'(0,\mu'')\frac{d\mu'}{\mu'}d\mu''\right], \tag{2.68}$$

and

$$U' = \overline{Q}'. \tag{2.69}$$

Performing these integrals, using equation (42), and solving for Q and U, we get:

$$Q = \frac{3(1-\mu^2)\phi(\mu)}{8(1+\delta^2\mu^2)} \int_0^1 P_2(\mu')I(0,\mu')d\mu', \tag{2.70}$$

and

$$U = \frac{3\delta\mu(1-\mu^2)\phi(\mu)}{8(1+\delta^2\mu^2)} \int_0^1 P_2(\mu')I(0,\mu')d\mu', \tag{2.71}$$

which are the same as the results obtained by Silant'ev (1979). The polarization at $\mu = 0$ is independent of δ, even for $\delta = \infty$, when the polarization is zero everywhere except $\mu = 0$ where it is equal to 9.137 per cent.